CHEMPHYSCHEM

DOI: 10.1002/cphc.200900557

An Alternative Approach to Quantify Partition Processes in Confined Environments: The Electrochemical Behavior of PRODAN in Unilamellar Vesicles**

Fernando Moyano, Patricia G. Molina, Juana J. Silber, Leonides Sereno,* and N. Mariano Correa*[a]

Herein, we investigate the behavior of the electroactive molecular probe 6-propionyl-2-dimethyl amino naphthalene (PRODAN) in large unilamellar vesicles (LUV) formed with the phospholipid 1,2-di-oleoyl-*sn*-glycero-3-phosphatidylcholine (DOPC) by using cyclic voltammetry (CV). The CV studies in pure water confirm our previous spectroscopic results that PRODAN self-aggregates due to its low water solubility. Moreover, the electrochemical results also reveal that the PRODAN aggregated species are non-electroactive within the studied electrochemical potential region. In DOPC LUV media, the redox behavior of PRODAN shows how the LUV bilayer interacts with PRODAN aggregated species to form PRODAN monomer species. Moreover, the electrochemical response of PRODAN allows us to propose a model for explaining the electrochemical experimental results and—in conjunction with our measurements—for calculating the value of the partition constant (K_p) of PRODAN between the water and LUV bilayer pseudophases. This value coincides with that obtained through an independent technique. Moreover, our electrochemical model allows us to calculate the diffusion coefficient (D) for the DOPC LUV, which coincides with the D value obtained through dynamic light scattering (DLS). Thus, our data clearly show that electrochemical measurements could be a powerful alternative approach to investigate the behavior of nonionic electroactive molecules embed in a confined environment such as the LUV bilayer. Moreover, we believe that this approach can be used to investigate the behavior of non-optical molecular drugs embedded in bilayer media.

1. Introduction

Organized molecular assemblies, such as vesicles or liposomes, can be considered as large cooperative units with characteristics that are very different from those of their individual structural units.[1] Vesicles are spherical aggregates formed by some amphiphilic compounds. The lipid bilayer surrounds an aqueous void volume which can be "loaded" with almost any variety of water-soluble marker molecules. Therefore, the vesicles may contain both lipophilic and water-soluble substances.[2,3] Phospholipids form the fundamental matrix of natural membranes and represent the environment in which many proteins and enzymes display their activity.[4] Results obtained from small unilamellar vesicles (SUVs) are often controversially discussed as model systems for cells because of their small size and bilayer defects due to their high curvature. For this reason, it is common to use large unilamellar vesicles (LUVs) to get closer to cell-like structures.[5–9]

On the other hand, interactions of small molecules with membranes are important issues in membrane biology. Understanding their role in modulating the structure and function of biological membranes requires the knowledge of the location of the molecules in the membranes.[10–13] Moreover, the study of electron-transfer process in such constrained environments can be useful since they can be used as models for understanding "natural" electron-transfer processes in biological membranes, for example, photosynthesis and cellular respiration. Recently,[12] we fully characterized the spectroscopic behavior of 6-propionyl-2-dimethyl amino naphthalene (PRODAN) in water as well as in LUVs of the phospholipid 1,2-di-oleoyl-*sn*-glycero-3-phosphatidylcholine (DOPC). The results from the absorption and emission bands reveal that PRODAN aggregates in water because of its low water solubility. In DOPC LUVs, PRODAN undergoes a partition process between the water bulk and the DOPC bilayer. We showed that the value of the partition constant, K_p, is large enough so that PRODAN in water can only be detected at DOPC concentrations (c_{DOPC}) below 0.15 mg mL^{-1}. PRODAN dissolved in LUVs at $c_{DOPC} >$ 1 mg mL^{-1} is completely incorporated in its monomer form.

With regards to electrochemical studies involving vesicle media, several efforts have been made to use these systems for the generation and amplification of electrochemical signals. For example, Baummer et al.[14] developed a new immunosensor for pesticide detection using a disposable system with vesicle-enhancement detection; Kwakye et al.[15] combined microelectronics and microfluidics with the simple and effective vesi-

[a] *Dr. F. Moyano, Dr. P. G. Molina, Prof. J. J. Silber, Prof. L. Sereno, Prof. N. M. Correa*
Departamento de Química, Universidad Nacional de Río Cuarto
Agencia Postal # 3, C.P. X5804BYA Río Cuarto (Argentina)
Fax: (+54) 358-4676233
E-mail: mcorrea@exa.unrc.edu.ar
lsereno@exa.unrc.edu.ar

[**] *PRODAN: 6-propionyl-2-dimethyl amino naphthalene*

Supporting information for this article is available on the WWW under http://dx.doi.org/10.1002/cphc.200900557

cle signal enhancement technology and designed a miniaturized electrochemical detection system to assemble and use for quantifying DNA and RNA molecules; Viswanathan et al.[16] reported a new approach for electrochemical immunoassay based on the utilization of encapsulated electrochemical signal-generating vesicles. They used ganglioside functionalized vesicles where potassium ferrocyanide is encapsulated and these vesicles act as highly specific recognition labels for the amplified detection to the cholera toxin. Another promising method in electrochemical sensing is the detection of molecules by using surface-modified electrodes containing vesicles or giants vesicles.[17–21] The adsorption and adhesion of vesicles play pivotal roles in many biological membrane processes. Also, as they can be doped with receptor moieties, they can mimic cell adhesion and can thus be used as targets to screen for membrane-active peptides. Moreover, vesicles provide the starting material for the formation of solid-supported lipid bilayers which are the desired matrix for membrane proteins in new sensor technologies.[18]

There are a few reports in which an electroactive molecule is encapsulated in the aqueous cavity of a vesicle and detected electrochemically upon lysis.[3,22,23] Very recently, Ikonen et al.[24] applied an electrochemical method to determine the vesicle–water partition coefficients of several water-soluble β-blockers. Particularly, electrochemical studies at liquid/liquid interfaces are a good tool for the determination of the partition constant, since they allow the control of the interfacial potential and the ionic distribution of the two phases. Thus, this study combines the rapid and easily controllable electrochemical method with the biomimetic capabilities of the vesicles.[25–27]

Cyclic voltammetry (CV) is one of the most versatile electroanalytical techniques for the study of electroactive species; thus, an electroactive probe would help in exploring the vesicular environment in which it will be solubilized. We previously applied this technique to perform a detailed study of the electrochemical behavior of the $Fe(CN)_6^{-4/-3}$ redox couple in water/sodium 1,4-bis-2-ethylhexylsulfosuccinate (AOT)/n-heptane reverse micelles using a Pt microelectrode due to the high resistivity of the media. In that work, we proposed a model that allowed us to determine the real concentration of the electroactive species under our experimental conditions and—from that value—also the diffusion coefficient of the AOT reverse micelles and their hydrodynamic radius. The values obtained are in very good agreement with the results obtained using other techniques, which clearly shows that the electrochemical measurements are a very powerful alternative approach for investigating organized media, such as reverse micelles.[28]

On the other hand, to the best of our knowledge, there are no studies focused on the properties of neutral molecules embed in vesicle bilayers which are based on their electrochemical response. An interesting event, which is worth being investigated, is the partitioning in water–liposome systems that molecular probes can experience since important results can be extrapolated to the drug-delivery process. The most common technique to achieve this goal is the use of the spectroscopic behavior of optical molecular probes dissolved in liposome media.[12] However, there are many drugs of biological interest which do not have accessible optical bands so that an optical approach might not be viable. Moreover, the common problem that arises when using spectroscopic methods in vesicle or liposome media is the inherent scattering due to the size of the aggregates. The scattering of the solution makes it almost impossible to investigate concentrated vesicle solutions (due to their turbidity) that are necessary for studying molecules whose partition-constant values are low. Electrochemical studies of electroactive molecules in bilayered media can be carried out as a viable alternative approach to eliminate these problems.

Herein, we have studied the electrochemical behavior of PRODAN in water—as well as in DOPC LUV media—by using the CV technique. The choice of the molecular probe is because it is a neutral, optical, electroactive and lipophilic molecule which can help us find out whether the electrochemical approach is viable to quantify the partitioning in water–vesicles systems. This came out because we previously investigated the PRODAN behavior in DOPC LUV.[12] In pure water, the electrochemical results confirm what was previously reported through the PRODAN photophysics,[12] namely, that PRODAN forms aggregated species due to its low water solubility (high lipophilicity[12]). The studies also reveal that the aggregate species are non-electroactive within the studied electrochemical potential region. In DOPC LUV media, the PRODAN redox behavior was investigated at different c_{DOPC}. Our electrochemical results confirm that PRODAN experiences a partition process between the water and the LUV bilayer pseudophases. Moreover, the results show how the LUV bilayer interacts with the PRODAN aggregated species to form PRODAN monomer species. This result seems to be quite important because it shows the bilayer de-aggregation property. We propose a model that allows us to explain the experimental results and, in conjunction with our measurements, to calculate the K_p value, which is similar to that obtained through the PRODAN photophysics studies previously reported in DOPC LUV media.[12] Also, our model makes it possible to calculate the diffusion coefficient (D) for the LUV, which coincides with that obtained through dynamic light scattering (DLS).

2. Results and Discussion

2.1. Electrochemical Behavior of PRODAN in Water

To the best of our knowledge, PRODAN electrooxidation has not been characterized in water so far, and the electrochemical mechanism of this reaction has only been reported in acetonitrile.[29] As DOPC LUVs are prepared in water, it is appropriate to start our work by investigating the electrochemical behavior of PRODAN in this solvent.

In acetonitrile, the voltammetric response of PRODAN corresponds to an irreversible electron-transfer process to give a radical cation. There is evidence of a chemical reaction after the electrochemical oxidation, corresponding to the reversible dimerization of the PRODAN radical cations.[29]

Figure 1 shows a typical cyclic voltammogram of PRODAN in water at $c_{PRODAN} = 6 \times 10^{-6}$ M and a scan rate of $v = 0.050$ Vs^{-1}.

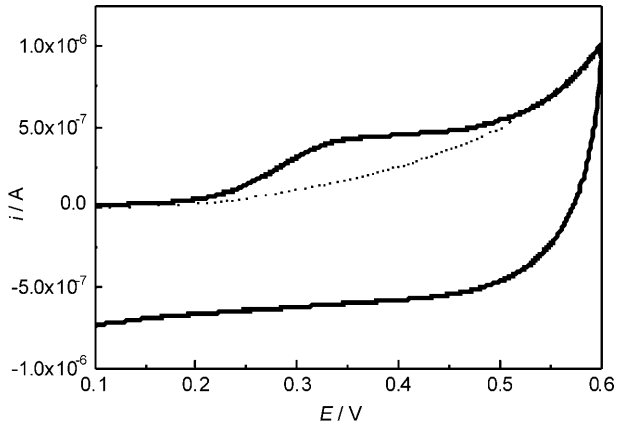

Figure 1. Cyclic voltammogram of PRODAN obtained in 0.1 M $LiClO_4$ (aq); $c_{PRODAN} = 6.0 \times 10^{-6}$ M; $v = 0.050$ V s^{-1}. The dotted line (••••) represents the background current.

An oxidation peak appears at 0.32 V and the corresponding cathodic peak is absent, which indicates that the electron-transfer process is complex[30] with a chemical reaction coupled to the initial electron transfer, as it was previously found in acetonitrile.[29]

The experimental cyclic voltammograms obtained at any v were digitally simulated using a BAS DigiSim® software (see Experimental Section). The best mechanism found for this fitting was the electrochemical–chemical (EC) one shown in Scheme 1.

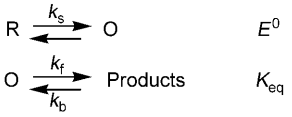

Scheme 1. Electrochemical–chemical (EC) mechanism.

In Scheme 1, R represents a PRODAN molecule while O is its radical cation, E^0 is the standard redox potential of the O/R couple, k_s is the charge-transfer constant of the Butler–Volmer equation,[31] k_f and k_b are the forward and backward kinetic first-order constants, and K_{eq} is the equilibrium constant of the chemical reaction. The parameter values obtained through the digital simulation are shown in Table S1 of the Supporting Information. It must be pointed out that a more detailed mechanistic study is not necessary for this work because we will use the PRODAN electrochemistry only as a tool to characterize the DOPC LUV.

The anodic-peak current (i_p) can be expressed by Equation (1):[30]

$$i_p = \chi_{(E)p} nF(nF/RT)^{1/2} AD^{1/2} c v^{1/2} \quad (1)$$

where n is the number of electrons (which is equal to one, as it was found in acetonitrile[29] and corroborated in the water experimental cyclic voltammogram fitting), F is Faraday's constant, A is the electrode area, D is the diffusion coefficient of PRODAN in water (D_{water}), c is the concentration of the electroactive species (in mol cm^{-3}), v is the scan rate, and $\chi_{(E)p}$ is the theoretical current function at the peak potential. A value of $\chi_{(E)p} = 0.441$ was obtained from the fitting of the experimental voltammograms shown in Figure 1 and using $D_{water} = 7 \times 10^{-6}$ cm^2 s^{-1} for PRODAN in water. The latter value was calculated from the D value in ACN[29] and the Stokes–Einstein equation.[31] It is known[12,29] that PRODAN does not aggregate in ACN but does in water.[12] Thus, the D_{water} value obtained for PRODAN corresponds to the diffusion coefficient of the monomer which is favored in the diluted solution used.

The plot of i_p versus $v^{1/2}$ shows a linear dependence at any PRODAN concentration (results not shown). These results demonstrate that the process in water is ruled by the diffusion of the electroactive species to the electrode.

To investigate the effect of PRODAN aggregation on the electrochemical response, we performed the same experiment but changing the PRODAN concentration.

Figure 2 shows the variation of the experimental i_p value with the analytical PRODAN concentration, c_{PRODAN}. The theoretical behavior of i_p versus c_{PRODAN}, predicted by Equation (1), is

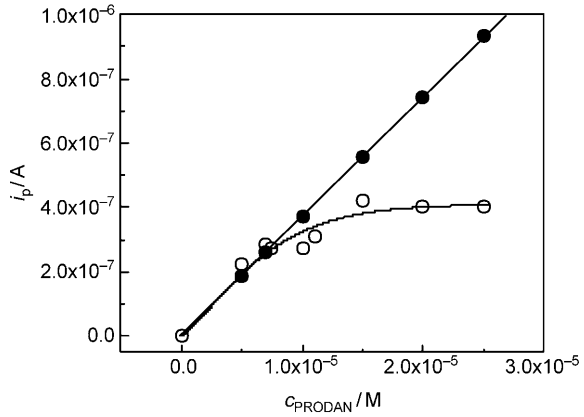

Figure 2. Dependence of i_p on c_{PRODAN} in 0.1 M $LiClO_4$ (aq); $v = 0.050$ V s^{-1}: Experimental (○) and theoretical (●) i_p values obtained from Equation (1).

also plotted for comparison. The data shows that the experimental i_p versus c_{PRODAN} profile is not linear as Equation (1) predicts. At low concentrations, both plots coincide but at $c_{PRODAN} \cong 1 \times 10^{-5}$ M, the feature deviates from the linear tendency. As PRODAN tends to aggregate in water at concentration above 1×10^{-5} M,[12] the results seem to suggest that only the PRODAN monomer is the electroactive species. Moreover, there was no other oxidation signal in the potential region studied. In other words, the electrochemical response of PRODAN in water is caused only by the monomer oxidation because the aggregate is not electroactive. This is not surprising since we have previously demonstrated[12] that the molar extinction coefficient of PRODAN for the charge-transfer electronic absorption band diminishes dramatically in water upon increasing the PRODAN concentration, which suggests that the intra-molecular charge-transfer process is inhibited by PRODAN

aggregation. In other words, electron transfer from the amino to the carbonyl group (lower epsilon value) is more difficult for the PRODAN aggregated species. Following with this thought, it is possible that PRODAN aggregation in water may also inhibit the electron-transfer process to the electrode.

Using the experimental i_p values shown in Figure 2 at every c_{PRODAN}, it is possible to obtain the "real" electroactive PRODAN concentration, that is, the monomer PRODAN concentration, c^m_{PRODAN}, through Equation (1). Figure 3 shows the dependence

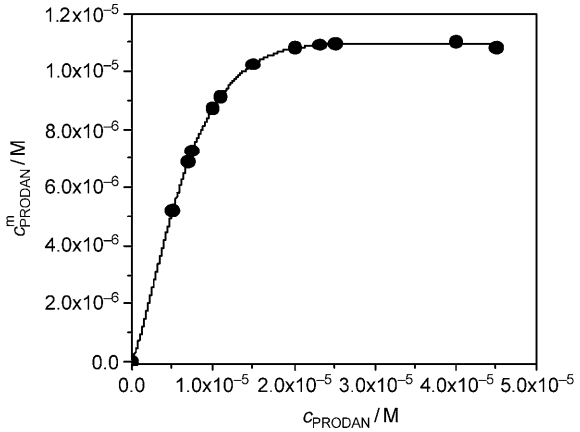

Figure 3. Dependence of c^m_{PRODAN} on c_{PRODAN}. The symbols (●) show the experimental results and the solid line (——) corresponds to the fitting to Equation (2). Fitting parameters: $B_1 = 1.11 \times 10^{-5}$ M, $B_2 = 1.24 \times 10^{-5}$ M, $k = 1.62 \times 10^5$ M^{-1}.

of c^m_{PRODAN} with c_{PRODAN}. As can be seen, when c_{PRODAN} is higher than 1.1×10^{-5} M, c^m_{PRODAN} is not the same as the analytical concentration because of the aggregation process invoked above. The best-fit function that describes the data shown in Figure 3 (solid line) is [Eq. (2)]:

$$c^m_{PRODAN} = B_1 - B_2 \exp(-k c_{PRODAN}) \quad (2)$$

where B_1, B_2, and k are the parameters that result from the best fitting with no physical or chemical significance. Thus, Equation (2) is an empirical equation that allows calculating the monomer PRODAN concentration at any analytical concentration.

2.2. Electrochemical Behavior of PRODAN in DOPC LUV

After characterizing the electrochemical behavior of PRODAN in water, we investigated the molecule in DOPC LUV media. Figure 4A shows cyclic voltammograms of PRODAN, 2×10^{-4} M, at different DOPC concentrations at $v = 0.10$ V s^{-1} while Figure S3 of the Supporting Information shows the corrected positive-sweep voltammograms. It must be noted that the PRODAN concentration used is more than ten times higher than the 10^{-6}–10^{-5} M concentration range used in pure water. The reason is that the electrochemical response of PRODAN is very weak in vesicle media at lower concentrations so that it is not possible to obtain a reliable i_p value. Accordingly, this indi-

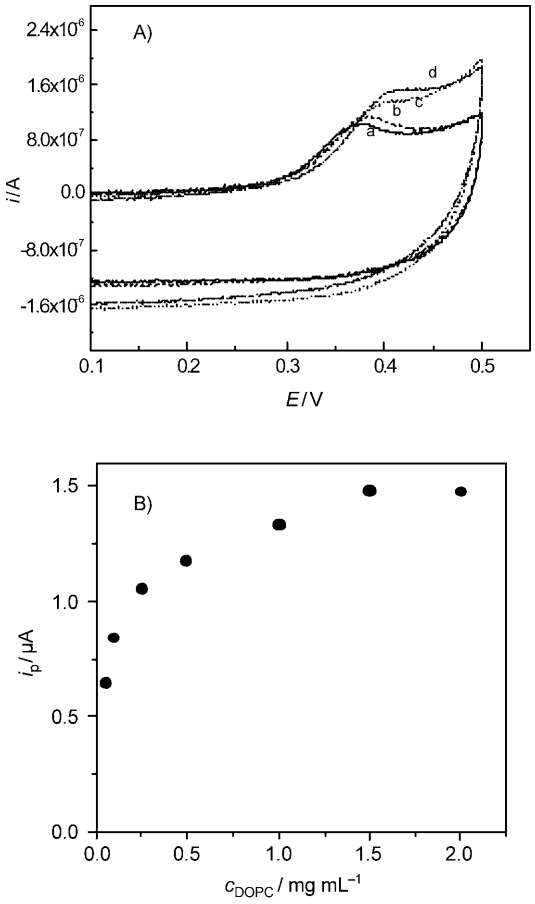

Figure 4. A) Cyclic voltammograms of PRODAN for different DOPC concentrations: a) 0.25, b) 0.50, c) 1.00, and d) 1.5 mg mL^{-1}. B) Dependence of i_p on the DOPC concentration; $c_{PRODAN} = 2.0 \times 10^{-4}$ M; $v = 0.100$ V s^{-1} in $c_{LiClO4} = 0.1$ M.

cates that in DOPC LUV media, the diffusion coefficient of the electroactive species is smaller than that in water, as we will explain below.

In LUV media, only the anodic peak is observed—with no cathodic counterpart (see Figure 4 A)—which indicates, again, that the electron-transfer process is complex with a chemical reaction coupled to the initial electron transfer, as it was previously found in acetonitrile[29] and in water. Figures S3 and S4 of the Supporting Information show the corrected voltammograms and corrected normalized voltammograms in water and DOPC LUV, respectively. It is clear that in DOPC LUV media, the profiles are the same as in water. Moreover, Figure S4 (Supporting Information) clearly supports the assumption that in both media the PRODAN oxidation mechanism is exactly the same. This comes out because the current function, $\chi_{(E)}$, has the same profile at any DOPC concentration and in water.

Although the profile in Figure 4A is analogous to that in water, two differences can be immediately observed: Despite the fact that c_{PRODAN} is constant, the anodic peak potential and the i_p values are higher than those in water—and both increase with the DOPC concentration (see Figures 4A,B and Figure S3 of the Supporting Information). The fact that the i_p value increases with the DOPC concentration (see Figure 4B)

shows that the concentration of the electroactive species in DOPC LUV depends on c_{DOPC}. We previously demonstrated[12] that PRODAN is incorporated into the DOPC LUV bilayer as a monomer; thus, the electroactive PRODAN specie in the vesicle media is the PRODAN monomer species. Moreover, the change in the peak potential probably reflects an increase in the concentration of the electroactive species and a change in the PRODAN environment. The latter change is expected since the molecule is incorporated into the LUV bilayer (as previously demonstrated).[12]

The question whether PRODAN is aggregated or not under the new electrochemical experimental conditions still remains. We have previously shown[12] that in DOPC LUV, PRODAN undergoes a partition process between the water bulk and the DOPC bilayer, and that PRODAN is incorporated only as a monomer into the bilayer as c_{DOPC} increases. The fluorescence studies in water have shown that a new emission band appears near $\lambda = 430$ nm as the PRODAN concentration increases. This signal corresponds to the emission band of the aggregate.[12] Since the experimental conditions used in ref. [12] are different from those used herein, we decided to extend the spectroscopic study to match the PRODAN concentration used in the electrochemical experiments. Also, we added supporting electrolyte to the solution. Figure 5 shows some of the experiments performed in this work on the emission spectra at $c_{PRODAN} = 2\times10^{-4}$ M and $c_{LiClO4} = 0.1$ M, varying c_{DOPC}. As it can be seen, at every DOPC concentration, the PRODAN aggregate band ($\lambda = 430$ nm) in water is present under these conditions, and the intensity of the aggregate band decreases as the DOPC concentration increases. For example, the $I_{\lambda max}/I_{\lambda 430\ nm}$ value ratio increases from 2.50 at [DOPC] = 0.05 mg mL^{-1} to 3.68 at [DOPC] = 0.5 mg mL^{-1}.

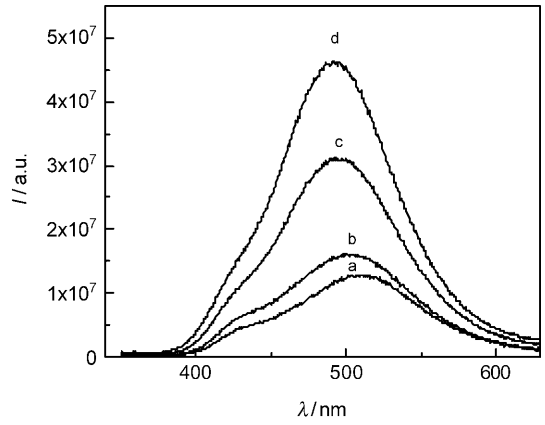

Figure 5. Emission spectra ($\lambda_{exc} = 322$ nm) of PRODAN at different DOPC concentrations: a) 0.05, b) 0.1, c) 0.25, and d) 0.5 mg mL^{-1}; $c_{PRODAN} = 2.0\times10^{-4}$ M in $c_{LiClO4} = 0.1$ M

In other words, under our experimental conditions the following PRODAN species are present, and their concentrations are c_{DOPC}-dependent (Scheme 2): PRODAN monomer (P^m), PRODAN aggregated (P^{agg}) in water, and PRODAN monomer bound to the DOPC LUV bilayer (P^{mb}). Moreover, our results in water demonstrate that only the PRODAN monomer species is electroactive.

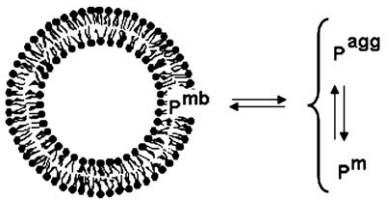

Scheme 2. PRODAN aggregation in water and distribution between the water and LUV bilayer pseudophases.

On the other hand, we investigated the dependence of i_p on the scan rate at different DOPC concentrations. Figure 6A shows typical results of i_p versus $v^{1/2}$ at different c_{DOPC} values and $c_{PRODAN} = 2\text{x}10^{-4}$ M. As it can be seen, there is a linear dependence at any DOPC concentration, which suggests that the process in DOPC LUV media is ruled by the diffusion of the electroactive species to the electrode as it was found in pure water. This linear dependence shown in Figure 6A also indicates that the PRODAN partition process in LUV media is fast, so it is not perturbed by the electrochemical technique. In other words, the kinetics of the PRODAN exchange between

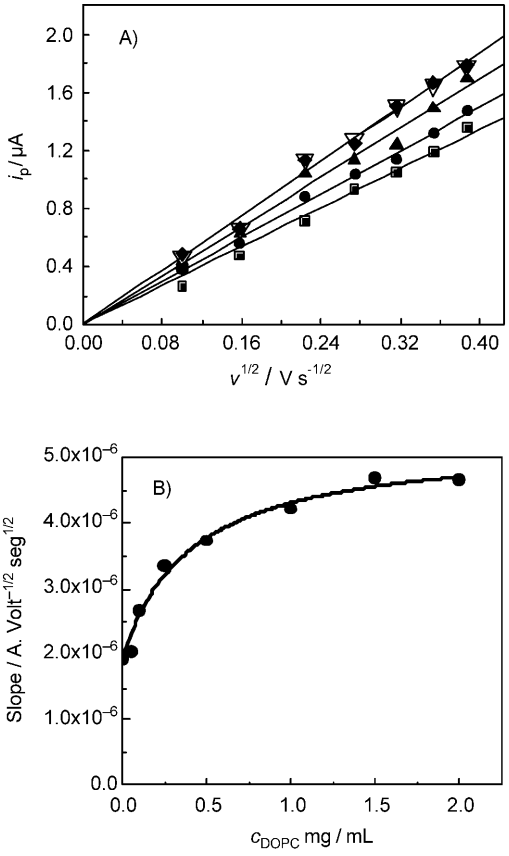

Figure 6. A) Dependence of i_p on $v^{1/2}$ at several DOPC concentrations: 0.25 mg mL^{-1} (■), 0.50 mg mL^{-1} (●), 1.00 mg mL^{-1} (▲), 1.5 mg mL^{-1} (▽), and 2.0 mg mL^{-1} (■); $c_{PRODAN} = 2.0\times10^{-4}$ M in $c_{LiClO4} = 0.1$ M. B) Dependence of the slope of the linear relations between i_p and $v^{1/2}$ on the DOPC concentration; $c_{PRODAN} = 2.0\times10^{-4}$ M in $c_{LiClO4} = 0.1$ M. The solid line (——) shows the fitting of the experimental data to Equation (14).

the two pseudophases is fast in comparison with the voltammetric time-scale.

Figure 6B shows the slopes of the linear fit obtained in Figure 6A for all the investigated DOPC concentrations. We also include the data for $c_{DOPC}=0$, which represent the slope obtained in pure water. We understand that this Figure 6B is a complete representation of the behavior of PRODAN in both pseudophases: water and the LUV bilayer. As the DOPC concentration increases, the slopes increase until they reach a constant value for c_{DOPC} around 2 mg mL^{-1} (result also shown in Figure 4B). Previous results obtained by spectroscopic methods[12] show that the value of the partition constant (K_p) of PRODAN is large enough so that PRODAN dissolved in LUV at $c_{DOPC} > 1$ mg mL^{-1} will exist completely incorporated in the bilayer. Our electrochemical data also suggest that the electrochemical response of PRODAN depends on its partition process, and that PRODAN is incorporated into the LUV bilayer only as a monomer; this is probably due to both its higher bilayer solubility[12] and its lower occupation number[32] at the DOPC bilayer, which make it difficult for two or more PRODAN molecules to interact. This result seems to be quite important because it shows a bilayer-de-aggregation property which may have potential applications for the preparation of dye lasers that require a non-interacting monomeric form of the dye.[32,33]

2.3. Electrochemical Model for the PRODAN Partition Process

To quantify the PRODAN partition process by using electrochemical techniques, it is necessary to propose a model which will have the following assumptions:

1) The equilibrium shown in Scheme 2, which represents the PRODAN aggregation process in water and its distribution process between the water and LUV bilayer pseudophases, are manifested simultaneously.
2) The PRODAN aggregation process in water has the same stoichiometry in the presence and absence of LUV. In addition, previous fluorescence anisotropy results show that these aggregates in pure water are far beyond the simple monomer–dimer equilibria.[12]
3) The electroactive species are the PRODAN monomer in the water pseudophase (P^m) and PRODAN incorporated into the LUV bilayer pseudophase (P^{mb}).
4) Both species are oxidized simultaneously at the same potential. This assumption is confirmed because Figure 4A and Figure S3 of the Supporting Information show only one voltammetric peak.

Keeping in mind these assumptions, Equation (3) can be formulated for the PRODAN aggregation in water:

$$\nu P^m \rightleftharpoons P^{agg} \quad (3)$$

where ν is the number of aggregated molecules. Although the value of ν is unknown,[12] this is not needed for our calculations since assumption 2 considers this constant value.

In LUV media, the PRODAN partition process between the DOPC LUV and water pseudophases is treated within the framework of the pseudophase model.[9,12] In this model, only two solubilization sites are considered, that is, the water and the vesicle interface, (i.e., all of the DOPC molecules). Thus, the distribution of PRODAN between the bilayer and the water pseudophase defined in Equation (4) is expressed in terms of the partition constant K_p shown in Equation (5):

$$P^{water} \rightleftharpoons P^{mb} \quad (4)$$

where P^{water} represent all the PRODAN species in water (monomer and aggregated):

$$K_p = \frac{c^{mb}_{PRODAN\#}}{c^{water}_{PRODAN}} \quad (5)$$

where $c^{water}{}_{PRODAN}$ is the total PRODAN concentration in water, that is, the sum of the monomer PRODAN concentration ($c^{m}{}_{PRODAN}$) and the aggregated PRODAN concentration ($c^{agg}{}_{PRODAN}$), and $c^{mb}{}_{PRODAN}{}^{\#}$ represents PRODAN bound to the bilayer in terms of local concentration. If $c^{mb}{}_{PRODAN}$ is the analytical (bulk) concentration of vesicle bound substrate, Equation (6) holds:

$$c^{mb}_{PRODAN}\# = \frac{c^{mb}_{PRODAN}}{c_{DOPC}} \quad (6)$$

the mass balance for the PRODAN is shown in Equation (7):

$$\begin{aligned} c_{PRODAN} &= c^{m}{}_{PRODAN} + \nu c^{agg}{}_{PRODAN} + c^{mb}{}_{PRODAN} \\ &= c^{water}{}_{PRODAN} + c^{mb}{}_{PRODAN} \end{aligned} \quad (7)$$

Hence, K_p can be expressed as [Eq. (8)]:

$$K_p = \frac{c^{mb}_{PRODAN}}{c^{water}_{PRODAN} C_{DOPC}} \quad (8)$$

where $c^{mb}{}_{PRODAN}$ and $c^{water}{}_{PRODAN}$ were defined before and c_{DOPC} is the total phospholipid concentration.

Taking Equations (7) and (8) into account, we obtain Equations (9) and (10):

$$c^{mb}{}_{PRODAN} = K_p c_{PRODAN} c_{DOPC}/(1 + K_p c_{DOPC}) \quad (9)$$

$$c^{water}{}_{PRODAN} = (c^{m}{}_{PRODAN} + \nu c^{agg}{}_{PRODAN}) = c_{PRODAN}/(1 + K_p c_{DOPC}) \quad (10)$$

Equation (9) allows the calculation of the concentration of electroactive PRODAN species in the DOPC LUV bilayer while Equation (10) can be used to calculate the PRODAN concentration in the water pseudophase (monomer and aggregated species).

To obtain the concentration of electroactive PRODAN species in water, $c^{m}{}_{PRODAN}$, we used the empirical Equation (2) for the electrochemical behavior of PRODAN in the water section and replaced c_{PRODAN} by $c^{water}{}_{PRODAN}$. Thus, Equation (11) was obtained:

$$c^{m}_{PRODAN} = B_1 - B_2\exp\{-k[c_{PRODAN}/(1 + K_p c_{DOPC})]\} \quad (11)$$

where B_1, B_2, and k are the parameters defined in Equation (2).

Because both electroactive species are oxidized at the same potential, the total peak current, i_{pTotal}, has two contributions, as shown in Equation (12):

$$i_{pTotal} = i_p^{Monomer}{}_{Water} + i_p^{PRODAN}{}_{LUV} \quad (12)$$

where $i_p^{Monomer}{}_{Water}$ and $i_p^{PRODAN}{}_{LUV}$ represent the peak current contributions from the PRODAN monomer in water and in the DOPC LUV bilayer, respectively. Each contribution can be expressed using Equation (1) and Equation (13) is deduced:

$$i_{pTotal} = \chi_{(E)p} nF\ (nF/RT)^{1/2} A[(D_{water})^{1/2} c^{m}_{PRODAN} + (D_{LUV})^{1/2} c^{mb}_{PRODAN}](v)^{1/2} \quad (13)$$

where D_{water} and D_{LUV} are the PRODAN diffusion coefficients in water (previously determined) and in the DOPC LUV pseudophases, respectively. All the other parameters were defined in Equation (1). Note that Equation (13) predicts a linear dependence between i_{pTotal} and $(v)^{1/2}$, as shown in Figure 6 A.

Finally, taking into account Equations (9), (11), and (13), we obtain Equation (14):

$$\left(\frac{i_p Total}{v^{1/2}}\right) = \text{Slope Eq. (13)} =$$
$$\chi_{(E)p} nF(nF/RT)^{1/2} A\{(D_{water})^{1/2}[B_1 - B_2\exp(-kc_{PRODAN}/(1 + K_p c_{DOPC})]$$
$$+(D_{LUV})^{1/2}[K_p c_{PRODAN} c_{DOPC}/(1 + K_p c_{DOPC})]\} \quad (14)$$

The experimental data shown in Figure 6 B were fitted to Equation (14) using a nonlinear regression method to determine the D_{LUV} and K_p values simultaneously. The values are gathered in Table 1, where experimental values obtained by using other techniques are also included for comparison. As it can be seen, the D_{LUV} values are within the experimental error, similar to those obtained by means of DLS. With regard to the K_p value obtained through Equation (14), a discussion is necessary. If we compare the value with that obtained by using emission spectroscopy[12] (see Table 1), it is clear that it is lower by a factor of about six. Since those are *apparent equilibrium constants*, and because the experimental conditions used before[12] are quite different, the value should be compared with the K_p value obtained through the data shown in Figure 5 where the spectroscopic experimental conditions match the electrochemical ones. Thus, to evaluate the K_p value, we now use the changes in the emission spectra with the DOPC concentration (Figure 5) following a procedure described previously.[9] The data are gathered in Table 1. It is evident that the K_p value obtained using Equation (14) is comparable (within the experimental error of both techniques) to that obtained by means of emission spectroscopy under the same experimental conditions.

Table 1. PRODAN partition constant, K_p, and PRODAN diffusion coefficient in DOPC LUV, D_{LUV}, obtained by using different techniques.

Technique	K_p [mL mg^{-1}]	D_{LUV} [cm^2 s^{-1}]
Cyclic Voltammetry	2.5 ± 0.3	$(6.1 \pm 1.2)\ 10^{-8}$
Emission Spectroscopy[a]	3.2 ± 0.9	-
Emission Spectroscopy[12]	16.4 ± 5	-
DLS	–	$(5.0 \pm 0.3)\ 10^{-8}$

[a] Value obtained from Figure 5 using identical experimental conditions: $c_{PRODAN} = 2.0 \times 10^{-4}$ M; $c_{LiClO4} = 0.1$ M.

Another interesting result is found if we compare the K_p value obtained in the DOPC LUV system with the values observed for the partition of PRODAN in other organized media, such as n-heptane/AOT/water reverse micelles,[34] where the molecular probe is much more soluble in the organic pseudophase (n-heptane) than in water. The K_p value in AOT reverse micelles is 2.5 M^{-1} whereas that in DOPC LUV media is 1875 M^{-1} (shown as 2.5 ± 0.3 mL mg^{-1}in Table 1). These results confirm that PRODAN prefers a hydrophobic environment to be located in the partition process between two different pseudophases. Moreover, the results show that this compound, which strongly self-aggregates, can be easily and quantitatively detected electrochemically in its monomeric form in the vesicles bilayer. These properties, added to the known enhancement that the bilayers have on the ionic-charge-specific molecular discrimination of charged electrochemical probes,[35] give a promising use of the techniques employed in this work not only to characterize interfaces but to understand undisclosed molecular recognition processes for non-ionic molecules.

3. Conclusions

We have investigated the electrochemical behavior of PRODAN in water and in DOPC LUV by means of cyclic voltammetry. In pure water, the results confirm that PRODAN self-aggregates due to its low water solubility, and that the aggregated species are non-electroactive. In DOPC LUV media, the redox behavior of PRODAN shows how the LUV bilayer interacts with the PRODAN aggregated species to form PRODAN monomer species—a result that demonstrates the bilayer-de-aggregation property in the studied system. Also, the PRODAN electrochemical response allows us to propose a model to explain the experimental results and—in conjunction with our measurements—calculate the PRODAN partition constant (K_p) value between the water and LUV bilayer pseudophases. Moreover, our model also allows calculation of the diffusion coefficient (D_{LUV}) for the DOPC LUV, which coincides with the D_{LUV} value obtained by using the DLS technique. Thus, our data clearly show that the electrochemical measurements could be a powerful alternative approach to investigate and characterize the behavior of lipophilic electroactive molecules embedded in a confined environment such as an LUV bilayer. Moreover, we believe that this approach can be used to investigate the behavior of non-optical molecular drugs embedded in bilayer media—a field that we are currently exploring.

Experimental Section

The lipid 1,2-di-oleoyl-*sn*-glycero-3-phosphatidylcholine (DOPC $T_c = -17.3\,^{\circ}C$[6,36]) in chloroform solution, obtained from Avanti Polar Lipids, Inc. (Alabaster Al, USA), and the fluorescent and electroactive probe 6-propionyl-2-dimethylaminonaphthalene, PRODAN, from Molecular Probes (Eugene Or), were used without further purification. At the temperature used in the experiences ($20 \pm 0.1\,^{\circ}C$), the DOPC LUV system is in a pure liquid-crystalline phase.[34]

The vesicle solution loaded with PRODAN was typically prepared as follows: the stock lipid solution was prepared by mixing the appropriate amount of DOPC and PRODAN in chloroform (Sintorgan HPLC). After the solvent was evaporated and the film was dried under reduced pressure, large MLVs were obtained by hydrating the dry lipid-dye film using 0.1 M $LiClO_4$ (FLUKA) water solution as supporting electrolyte, through mixing (Vortex–2-Genie) for about 5 min at room temperature. The resulting solution of MLVs had the desired lipid and PRODAN concentrations. To prepare LUVs, the MLV suspension was extruded ten times (Extruder, Lipex biomembranes) through two stacked polycarbonate filters of pore size 200 nm under nitrogen pressure up to 3.4 atm. The monodispersity of the LUV size achieved through this technique was previously checked.[6,7,37] The unilamellar nature of the pure DOPC vesicles prepared by using the extrusion method[37] was previously confirmed[4,5,7,38] by measuring the extent of quenching by Mn^{+2} of their ^{31}P NMR signals.[39] All samples were used immediately after preparation. Ultrapure water was obtained from a Labconco equipment model 90901–01.

The absorption spectra were measured using a Shimadzu 2401 equipment at $(20 \pm 0.1)\,^{\circ}C$. A Spex fluoromax apparatus was employed for the fluorescent measurements. Corrected fluorescence spectra were obtained using the correction file provided by the manufacturer. The path length used in the absorption and emission experiments was 1 cm. λ_{max} was measured by taking the midpoint between the two positions of the spectrum where the absorbance was equal to 0.9 A_{max}. The uncertainties in λ_{max} were about 0.1 nm. To subtract the background contribution of the absorption and emission spectra, samples of the same concentrations of phospholipids were prepared omitting the addition of the probes.

The diameters of the LUV were determined by dynamic light scattering (DLS, Malvern 4700 with goniometer and 7132 correlator) with an argon-ion laser operating at 488 nm. All the measurements were carried out at a scattering angle of 90° at a temperature of $20 \pm 0.1\,^{\circ}C$. The DLS experiments show that the polidispersity of the LUV size is less than 5%.

An AutoLab PGSTAT 30 potentiostat, controlled by the GPES 4.8 software, was employed for the CV measurements. The cyclic voltammograms were obtained in the range of 10 to 150 $mV\,s^{-1}$. The working electrode was a Pt wire (Area = 0.251 cm^2) constructed in our laboratory, as previously described.[40] It was polished, sonicated, copiously rinsed with distilled water, and dried prior to use until reproducible surfaces were obtained. The counter electrode was a platinum foil of large area ($\approx 2\,cm^2$). A freshly prepared Ag/AgCl quasi-reference electrode was used. All the experiments were performed under a purified nitrogen atmosphere at $T = (20 \pm 0.1)\,^{\circ}C$. The Ohmic drop was carefully compensated by using the positive-feedback technique.

OriginPro 7.0 was used for analysis and calculations. The digital simulations of the voltammograms (in water) for the EC mechanism shown in Scheme 1 were performed using the program DigiSim® version 2.1 (Bioanalytical Systems, West Lafayette IN) where the algorithms of Feldberg and Rudolph are described in ref. [41]. The fast implicit finite difference method was implemented with an exponential expansion of the spatial grid and with default values of the DigiSim software. To avoid any divergent behavior during the adjustment, we assumed—as recommended by the authors of the software—that the diffusion coefficients of all the species in the mechanism are identical. The experimental voltammograms (after subtracting the background current) and the digital simulation are shown in Figures 1SA and 1SB in the Supporting Information. The average values of the parameters obtained from the simulations are shown in Table 1S of the Supporting Information, and they are in good agreement with the experimental results obtained at seven scan rates in the 0.010–0.150 $V\,s^{-1}$ range.

To perform the calculations derived from the voltammograms shown herein, only the anodic current was used after subtracting the background current. These background-corrected cyclic voltammograms are shown in Figures S2 and S3 of the Supporting Information.

Acknowledgements

Financial support from the Consejo Nacional de Investigaciones Científicas y Técnicas (CONICET), the Universidad Nacional de Río Cuarto, the Agencia Nacional de Promoción Científica y Técnica, and the Agencia Córdoba Ciencia is gratefully acknowledged. JJS, NMC and PGM hold a research position at CONICET. FM thanks CONICET for a research fellowship.

Keywords: cyclic voltammetry · electrochemistry · nanostructures · partition constants · vesicles

[1] A. Chattopadhyay, S. Mukherjee, *Biochemistry* **1993**, *32*, 3804.
[2] M. Kępczyński, K. Nawalani, B. Jachimska, M. Romek, M. Nowakowska, *Colloid Surf. B* **2006**, *49*, 22.
[3] R. M. Kannuck, J. M. Bellama, R. A. Durst, *Anal. Chem.* **1988**, *60*, 142.
[4] T. Parasassi, G. De Stasio, A. D'Ubaldo, E. Gratton, *Biophys. J.* **1990**, *57*, 1179.
[5] S. Rex, *Biophys. Chem.* **1996**, *58*, 75.
[6] N. M. Correa, Z. A. Schelly, *Langmuir* **1998**, *14*, 5802.
[7] N. M. Correa, Z. A. Schelly, *J. Phys. Chem. B* **1998**, *102*, 9319.
[8] N. M. Correa, Z. A. Schelly, H. Zhang, *J. Am. Chem. Soc.* **2000**, *122*, 6432.
[9] F. Moyano, J. J. Silber, N. M. Correa, *J. Colloid Interface Sci.* **2008**, *317*, 332.
[10] P. L.-G. Chong, S. Capes, P. T. T. Wong, *Biochemistry* **1989**, *28*, 8358.
[11] J. Seelig, P. M. McDonald, P. G. Scherer, *Biochemistry* **1987**, *26*, 7535.
[12] F. Moyano, M. A. Biasutti, J. J. Silber, N. M. Correa, *J. Phys. Chem. B* **2006**, *110*, 11838.
[13] P. H. Devaux, M. Signeuret, *Biochim. Biophys. Acta* **1985**, *822*, 63.
[14] A. J. Bäumner, R. D. Schmid, *Biosens. Bioelectron.* **1998**, *13*, 519.
[15] S. Kwakye, V. N. Goral, A. J. Baeumner, *Biosens. Biolectron.* **2006**, *21*, 2217.
[16] S. Viswanathan, L.-C. Wu, M.-R. Huang, J.-A. Ho, *Anal. Chem.* **2006**, *78*, 1115.
[17] J. A. P. Piedade, M. Mano, M. C. Pedroso de Lima, T. S. Oretskaya, A. M. Oliveira-Brett, *Biosens. Bioelectron.* **2004**, *20*, 975.
[18] A. Sapper, B. Reiss, A. Janshoff, J. Wegener, *Langmuir,* **2006**, *22*, 676.
[19] J. A. Bard, X. Li, W. Zhan, *Biosens. Bioelectron.* **2006**, *22*, 461.
[20] V. Agmo Hernández, F. Scholz, *Langmuir,* **2006**, *22*, 10723.
[21] D. Grieshaber, R. MacKenzie, J. Voros, E. Reimhult, *Sensors* **2008**, *8*, 1400.
[22] P. D' Orazio, G. Rechnitz, *Anal. Chem.* **1977**, *49*, 2083.
[23] A. T. Jenkins, J. A. Olds, *Chem. Commun.* **2004**, 2106.
[24] M. Ikonen, L. Murtomäki, K. Kontturi, *J. Electroanal. Chem.* **2007**, *602*, 189.

[25] C. Letizia, P. Andreozzi, A. Scipioni, C. La Mesa, A. Bonincontro, E. Spignone, *J. Phys. Chem. B* **2007**, *111*, 898.
[26] A. Bonincontro, C. La Mesa, C. Proietti, G. Risuleo, *Biomacromolecules* **2007**, *8*, 1824.
[27] A. Bonincontro, M. Falivene, C. La Mesa, G. Risuleo, M. Ruiz Peña, *Langmuir,* **2008**, *24*, 1973.
[28] P. G. Molina, J. J. Silber, N. M. Correa, L. Sereno, *J. Phys. Chem. C* **2007**, *111*, 4269.
[29] M. B. Moressi, M. A. Zón, H. Fernández, *Can. J. Chem.* **2002**, *80*, 1232.
[30] R. S. Nicholson, I. Shain, *Anal. Chem.* **1964**, *36*, 706.
[31] A. J. Bard, L. R. Faulkner, *Electrochemical Methods: Fundamentals and Applications*, 2nd Ed., Wiley, New York, **2001**.
[32] R. D. Falcone, N. M. Correa, M. A. Biasutti, J. J. Silber, *Langmuir,* **2002**, *18*, 2039.
[33] S. Gupta, L. Mukhopadhyay, *Indian J. Chem.* **1997**, *35*, 31.
[34] M. Novaira, M. A. Biasutti, J. J. Silber, N. M. Correa, *J. Phys. Chem. B* **2007**, *111*, 748.
[35] M. Twardowski, R. G. Nuzzo, *Langmuir* **2004**, *20*, 175.
[36] R. N. A. H. Lewis, R. N. McElhaney in *The Structure of Biological Membranes*, (Ed.: P. Yeagle), CRC Press, Boca Raton, **1992**.
[37] L. D. Mayer, M. J. Hope, P. R. Cullis, *Biocchim. Biophys. Acta,* **1986**, *858*, 161.
[38] N. Asgharian, X. Wu, R. L. Meline, B. Derecskei, H. Cheng, Z. A. Schelly, *J. Mol. Liq.* **1997**, *72*, 315.
[39] M. J. Hope, M. B. Bally, G. Webb, P. R. Cullis, *Biocchim. Biophys. Acta,* **1985**, *812*, 55.
[40] M. A. Zon, H. Fernandez, L. Sereno, J. J. Silber, *Electrochim. Acta,* **1987**, *32*, 71.
[41] M. Rudolph, D. P. Reddy, S. W. Feldberg, *Anal. Chem.* **1994**, *66*, 589A.

Received: July 16, 2009
Published online on November 26, 2009

